J|A|C|S ARTICLES

Published on Web 01/20/2009

Magnetism of C Adatoms on BN Nanostructures: Implications for Functional Nanodevices

Jia Li,[†] Gang Zhou,[†] Ying Chen,[‡] Bing-Lin Gu,[†] and Wenhui Duan*[,†]

Department of Physics, Tsinghua University, Beijing 100084, People's Republic of China, and Department of Electronic Materials Engineering, Research School of Physical Sciences and Engineering, The Australian National University, Canberra, ACT 0200, Australia

Received July 18, 2008; E-mail: dwh@phys.tsinghua.edu.cn

Abstract: Spin-polarized density functional calculations reveal that magnetism can be induced by carbon adatoms on boron nitride nanotubes (BNNTs) and BN hexagonal sheets. As a result of the localization of impurity states, these hybrid sp-electron systems are spin-polarized, with a local magnetic moment of 2.0 μ_B per C adatom regardless of the tube diameter and the bonding between the C atom and the BNNTs/BN sheets. An analysis of orbital hybridization indicates that two valence electrons participate in the bonding and the remaining two electrons of the C adatom are confined at the adsorption site and contribute to the magnetism accordingly. The effective interaction distance between the C-induced magnetic moments is evaluated. In terms of the diffusion barrier and the adsorption energy of C adatoms on the BN nanotubes/sheets, a fabrication method for BN−C-based functional nanodevices is proposed, and a series of virtual building blocks for functional devices are illustrated.

I. Introduction

In the past decade, boron nitride nanotubes (BNNTs) have received increasing attention.[1] Because of their high thermal and chemical stabilities, BNNTs are expected to have enormous potential applications as protective shields of some nanomaterials, nanostructured composite materials, and nanoscale electronic devices, even at high temperatures and/or in hazardous environments.[2,3] Recently, single-layer (SL) hexagonal BN (*h*-BN) sheets have also been studied by many researchers with great enthusiasm because they can be easily grown by chemical vapor deposition on transition metals[4] and are proposed as an alternative to graphene for plane electronics, where the lithography technique can be conveniently applied. The wide band gap of BN nanomaterials, however, is a substantial obstacle for their applications in electronics. In numerous efforts to reduce the band gap, the doping of BNNTs, especially with carbon, was proposed and implemented early on,[1] and the resulting effects are pronounced (e.g., the band gap of the system is reduced to ∼1 eV as a result of substitutional C doping[5]).

On the other hand, magnetism at the nanoscale is an exciting emerging research field of both fundamental and applied interest. In general, an atom with unsaturated valence electrons or dangling bonds (DBs) could lead to the generation of a net local magnetic moment. This, however, neither guarantees the appearance of a net moment nor assures the existence of ferromagnetism. For instance, both open armchair C and BN nanotubes have some DBs at the open ends; however, they are nonmagnetic, and no local magnetic moments are induced.[6,7] For any doped systems, a crucial issue for their applications in spintronic devices is whether local magnetic moments induced by the defect states can lead to a collective magnetism by the long-range magnetic coupling, which is an essential requirement for any spintronic application. However, this critical issue, as well as its implications for practical applications, was often overlooked in previous studies on doping-induced magnetism of nanostructures.

At present, it is still a great challenge to find suitable candidate materials for spintronic devices from various sp-electron nanomaterials such as C or BN systems.[8] Previous theoretical works have suggested that magnetism may occur in BN/C heterostruc-

[†] Tsinghua University.
[‡] The Australian National University.

(1) Golberg, D.; Bando, Y.; Tang, C. C.; Zhi, C. Y. *Adv. Mater.* **2007**, *19*, 2413.
(2) (a) Rubio, A.; Corkill, J. L.; Cohen, M. L. *Phys. Rev. B* **1994**, *49*, 5081. (b) Blase, X.; Rubio, A.; Louie, S. G.; Cohen, M. L. *Europhys. Lett.* **1994**, *28*, 335.
(3) Chen, Y.; Zou, J.; Campbell, S. J.; Caer, G. L. *Appl. Phys. Lett.* **2004**, *84*, 2430.
(4) (a) Corso, M.; Greber, T.; Osterwalder, J. *Surf. Sci.* **2005**, *577*, L78. (b) Morscher, M.; Corso, M.; Greber, T.; Osterwalder, J. *Surf. Sci.* **2006**, *600*, 3280. (c) Goriachko, A.; He, Y. B.; Knapp, M.; Over, H.; Corso, M.; Brugger, T.; Berner, S.; Osterwalder, J; Greber, T. *Langmuir* **2007**, *23*, 2928.
(5) (a) Golberg, D.; Bando, Y.; Dorozhkin, P.; Dong, Z.-C. *MRS Bull.* **2004**, *29*, 38. (b) Golberg, D.; Dorozhkin, P. S.; Bando, Y.; Dong, Z.-C.; Tang, C. C.; Uemura, Y.; Grobert, N.; Reyes-Reyes, M.; Terrones, H.; Terrones, M. *Appl. Phys. A: Mater. Sci. Process.* **2003**, *76*, 499. (c) Zhi, C. Y.; Guo, J. D.; Bai, X. D.; Wang, E. G. *J. Appl. Phys.* **2002**, *91*, 5325.
(6) Kim, Y.-H.; Choi, J.; Chang, K. J.; Tománek, D. *Phys. Rev. B* **2003**, *68*, 125420.
(7) (a) Hao, S. G.; Zhou, G.; Duan, W. H.; Wu, J.; Gu, B.-L. *J. Am. Chem. Soc.* **2006**, *128*, 8453. (b) Zhou, G.; Duan, W. H. *Chem. Phys. Lett.* **2007**, *437*, 83.
(8) (a) Makarova, T. L.; Sundqvist, B.; Höhne, R.; Esquinazi, P.; Kopelevich, Y.; Scharff, P.; Davydov, V. A.; Kashevarova, L. S.; Rakhmanina, A. V. *Nature* **2001**, *413*, 716. (b) Coey, J. M. D.; Venkatesan, M.; Fitzgerald, C. B.; Douvalis, A. P.; Sanders, I. S. *Nature* **2002**, *420*, 156. (c) Esquinazi, P.; Spemann, D.; Höhne, R.; Setzer, A.; Han, K.-H.; Butz, T. *Phys. Rev. Lett.* **2003**, *91*, 227201. (d) Ohldag, H.; Tyliszczak, T.; Höhne, R.; Spemann, D.; Esquinazi, P.; Ungureanu, M.; Butz, T. *Phys. Rev. Lett.* **2007**, *98*, 187204.

10.1021/ja805632p CCC: $40.75

tures[9] and that local magnetic moments can be achieved by adsorption of F on BNNTs.[10] In an effort to elucidate the origin of magnetism in pure-carbon systems,[11] theoretical studies have demonstrated the role of C adatoms.[12] From the structural similarity between carbon nanotubes (CNTs)/graphene and BNNTs/*h*-BN sheets, one can expect that similar magnetic phenomena would emerge in BNNTs and *h*-BN sheets with the help of C adatoms, while the pronounced difference between C and BN nanostructures in electronic structures would lead to different characteristic of the induced magnetism. This speculation could be significant for future spintronics applications where the spin of the electron instead of its charge is used as the information carrier,[13] because it endows ordinary BN nanomaterials with the unexpected magnetic property and then could offer exciting opportunities for the preparation of high-temperature ferromagnetic semiconductors. In particular, it is now possible to fabricate unique integrated nanostructures via C adsorption on the as-grown or growing BN sheets and nanotubes, because the C atoms can be stably doped via substitution or chemical addition into BN nanostructures in experiments.[1,14] Therefore, a comprehensive study of the whole process (i.e., C adsorption and diffusion on *h*-BN sheets and BNNTs) is necessary and important for gaining insight into the mechanism of magnetism and understanding of the fabrication of functional BN−C nanostructures.

In this work, with spin-polarized density functional theory (DFT), we investigated the adsorption and diffusion of C adatoms on BN nanostructures (i.e., nanotubes and sheets) and found that a single C adatom on an *h*-BN sheet and on BNNTs induces a local magnetic moment of $2.0\mu_B$, regardless of adsorption geometry and tube diameter. This characteristic is distinctly different from that for C adatoms on graphene and CNTs.[12] Our orbital hybridization analysis shows that the induced spin polarization and local magnetic moment mainly originate from the strong localization of the unpaired electrons of the C adatoms. With the injection of negative charges, such C−BN hybrid structures exhibit substantial collective magnetism. On the other hand, the diffusion of C atoms on the BNNTs is demonstrated to be predominately along the tube axis, facilitating the fabrication of BN/C superlattices or heterojunctions. From the unique adsorption and diffusion properties, we explore the feasibility of synthesizing BN−C-based functional devices by C adsorption on BN nanostructures.

II. Methods and Models

We studied the adsorption and diffusion of C atoms on *h*-BN sheets and zigzag single-walled BNNTs [i.e., (8,0), (12,0), (16,0), and (20,0) ones], since many experiments have shown that BNNTs prefer a nonhelical or zigzag orientation during growth.[15] All of the calculations were performed using the DMol^3 package,[16] which implements local-orbital spin-polarized DFT. The generalized gradient approximation combining the Perdew−Wang correlation functional with the Becke exchange functional was utilized.[17] The double-numerical basis set with polarized functions was employed in all of the calculations. We adopted a hexagonal $3 \times 3 \times 1$ supercell for an *h*-BN sheet and a tetragonal $1 \times 1 \times 2$ supercell for the BNNTs. In the supercells, a vacuum region of $\sim$10 Å was employed to eliminate the tube−tube or sheet−sheet interactions. The $7 \times 7 \times 1$ and $1 \times 1 \times 5$ Monkhorst−Pack **k**-point meshes[18] were used to sample the Brillouin zones for the *h*-BN sheet and BNNT, respectively, which are found to yield an meV per atom convergence of the total energy. In the study of the adsorption of C atoms, we considered on-top sites of B and N atoms, bridge sites between B and N atoms, and the center site above the hexagon as the initial adsorption sites, and the whole system was allowed to relax fully until all of the force components on the ions were less than 10^{-3} au. Furthermore, we used the linear/quadratic synchronous transit (LST/QST) method[19] to calculate the diffusion barriers of the C adatom on the tube and the *h*-BN sheet. Frequency calculations were used to validate all of the transition states, each of which should have only one imaginary frequency. The adsorption energy E_{ads} was obtained from the following expression:

$$E_{ads} = E_{tot}[\mathrm{BN}] + E_{tot}[\mathrm{C}] - E_{tot}[\mathrm{BN+C}] \quad (1)$$

where E_{tot}[BN], E_{tot}[C], and E_{tot}[BN + C] are the total energies of the *h*-BN sheet or BNNTs, the free C atom in the triplet state, and the C-adsorbed *h*-BN sheet or BNNTs, respectively. Actually, the van der Waals (vdW) interaction has a certain effect on the adsorption and diffusion of adatoms (e.g., a slightly smaller equilibrium distance between the C adatom and the BN nanostructure), especially before bonding between adatoms and BN nanostructures. Since the influence of the nonbonding vdW interactions on geometrical optimization is very small, no special treatment of vdW force was considered in this work.

III. Results and Discussion

Our calculations show that similar to the cases of C adatoms on graphene and CNTs,[12,20] the C adatom on an *h*-BN sheet and on BNNTs prefers to stay at a bridgelike site of the B−N bond (Figure 1). For zigzag nanotubes, there exist two kinds of bridgelike adsorption structures: one is "perpendicular" to the tube axis (denoted as the Per-Bri structure), and the other is parallel to the tube axis (denoted as the Par-Bri structure). From Table 1, we can see that for all of the BNNTs, the adsorption energy of the C adatom in the Per-Bri site is always larger than that in the Par-Bri site. As the tube diameter increases, the adsorption energy decreases monotonically to approach the value for the *h*-BN sheet, which can be regarded as a limiting case of a BNNT (i.e., a BNNT with infinite radius).

For pristine BNNTs, the B−N bond perpendicular to the tube axis (Per B−N bond) is longer and generally a bit weaker than the B−N bond parallel to the tube axis (Par B−N bond), as

(9) (a) Okada, S.; Oshiyama, A. *Phys. Rev. Lett.* **2001**, *87*, 146803. (b) Choi, J.; Kim, Y.; Chang, K. J.; Tomanek, D. *Phys. Rev. B* **2003**, *67*, 125421. (c) Li, X. Y.; Yang, W.; Liu, B. *Nano Lett.* **2007**, *7*, 3709.
(10) Li, F.; Zhu, Z. H.; Yao, X. D.; Lu, G. Q.; Zhao, M. W.; Xia, Y. Y.; Chen, Y. *Appl. Phys. Lett.* **2008**, *92*, 102515.
(11) *Carbon-Based Magnetism*; Makarova, T., Palacio, F., Eds.; Elsevier: Amsterdam, 2006; Chapter 24.
(12) (a) Lehtinen, P. O.; Foster, A. S.; Ayuela, A.; Krasheninnikov, A.; Nordlund, K.; Nieminen, R. M. *Phys. Rev. Lett.* **2003**, *91*, 017202. (b) Lehtinen, P. O.; Foster, A. S.; Ayuela, A.; Vehviläinen, T. T.; Nieminen, R. M. *Phys. Rev. B* **2004**, *69*, 155422.
(13) Wolf, S. A.; Awschalom, D. D.; Buhrman, R. A.; Daughton, J. M.; von Molnar, S.; Roukes, M. L.; Chtchelkanova, A. Y.; Treger, D. M. *Science* **2001**, *294*, 1488.
(14) Kim, S. Y.; Park, J.; Choi, H. C.; Ahn, J. P.; Hou, J. Q.; Kang, H. S. *J. Am. Chem. Soc.* **2007**, *129*, 1705.
(15) (a) Golberg, D.; Han, W.; Bando, Y.; Bourgeois, L.; Kurashima, K.; Sato, T. *J. Appl. Phys.* **1999**, *86*, 2364. (b) Golberg, D.; Bando, Y.; Kurashima, K.; Sato, T. *Chem. Phys. Lett.* **2000**, *323*, 185.
(16) Delley, B. *J. Chem. Phys.* **1990**, *92*, 508; Delley, B. *J. Chem. Phys.* **2000**, *113*, 7756; DMol^3 is available from Accelrys.
(17) (a) Perdew, J. P.; Wang, Y. *Phys. Rev. B* **1992**, *45*, 13244. (b) Becke, A. D. *Phys. Rev. A* **1988**, *38*, 3098.
(18) Monkhorst, H. J.; Pack, J. D. *Phys. Rev. B* **1976**, *13*, 5188.
(19) (a) Govind, N.; Petersen, M.; Fitzgerald, G.; King-Smith, D.; Andzelm, J. *Comput. Mater. Sci.* **2003**, *28*, 250. (b) Halgren, T. A.; Lipscomb, W. N. *Chem. Phys. Lett.* **1977**, *49*, 225.
(20) Krasheninnikov, A. V.; Nordlund, K.; Lehtinen, P. O.; Foster, A. S.; Ayuela, A.; Nieminen, R. M. *Phys. Rev. B* **2004**, *69*, 073402.

Table 1. Calculated Adsorption Energies (E_{ads}) of the C Adatom and Distances between the B and N Adjacent to the C Adatom (d_{B-N}), between B and C (d_{B-C}), and between N and C (d_{N-C}) for the *h*-BN sheet and (8,0), (12,0), (16,0) and (20,0) BNNTs (Values in Parentheses Are the Corresponding Values for the Pristine *h*-BN sheet and BNNTs)

		E_{ads} (eV)		d_{B-N} (Å)		d_{B-C} (Å)		d_{N-C} (Å)	
nanotube	diameter (Å)	Par-Bri	Per-Bri	Par-Bri	Per-Bri	Par-Bri	Per-Bri	Par-Bri	Per-Bri
(8,0)	6.504	1.36	2.08	1.652 (1.455)	2.339 (1.465)	1.604	1.533	1.489	1.384
(12,0)	9.688	1.15	1.71	1.615 (1.451)	2.314 (1.458)	1.634	1.531	1.516	1.383
(16,0)	12.892	1.07	1.54	1.602 (1.451)	2.300 (1.457)	1.649	1.529	1.530	1.382
(20,0)	16.114	1.03	1.44	1.595 (1.451)	2.293 (1.456)	1.661	1.528	1.540	1.381
BN sheet	∞	0.95		1.546 (1.455)		1.745		1.617	

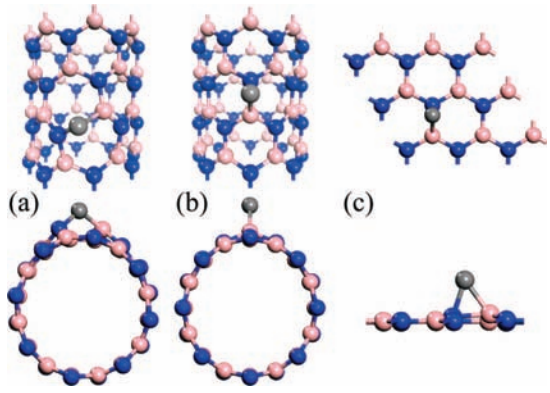

Figure 1. Optimized geometries of the C-adsorbed (8,0) BNNT (a, b) and SL *h*-BN sheet (c). In (a) and (b), the C adatom occupies B−N bridge sites "perpendicular" and "parallel" to the tube-axis, respectively. Pink, blue, and gray balls represent B, N, and C atoms, respectively.

shown in Table 1. This is compatible with the fact that the $\sigma-\pi$ hybridization of the Per B−N bond is more pronounced because of the upshift of the σ states induced by the curvature. When the C atom approaches the Per-Bri site, two polar covalent bonds are formed via hybridization of the sp^2 hybrid orbitals of the C adatom and the upshifted σ states of the adjacent B and N atoms. Meanwhile, the C atom pushes the two adjacent B and N atoms apart to at least 2.20 Å, which is far larger than the standard B−N bond length of 1.46 Å in the BNNT. Thus, the original Per B−N bond is considered to be "broken". Such broken Per-Bri bonds have previously been found in both C-adsorbed CNTs and O-doped BNNTs.[12,20,21] In contrast, for C adsorption at the Par-Bri site, the bonds of B and N with C present the characteristic of sp^2-sp^3 hybridization, so the mixed-hybrid bond is weaker in nature than the complete sp^2-hybrid one in the C-adsorbed Per-Bri structure. In addition, regardless of tube diameter, the C-adsorbed B−N bond length d_{B-N} in the Par-Bri structure is always ∼1.60 Å, which is larger than the value of 1.45 Å for the pristine BNNTs (see Table 1). Consequently, the C adatom in the Par-Bri structure merely leads to some weakening or deformation of the associated B−N bond. In a word, because of the curvature effect, the adsorption mechanisms are different for C atoms at the Per-Bri and Par-Bri sites of zigzag BNNTs, corresponding to different changes (i.e., formation or breaking) of chemical bonds upon C adsorption on the BNNTs; the results suggest that the Per-Bri site is more energetically favorable for C adsorption. On the other hand, as the tube diameter increases, the adsorption energy difference between the Per-Bri and Par-Bri structures gradually decreases (see Table 1). It is expected that when the tube diameter is large enough, the probabilities for adsorption of C adatoms at the Per-Bri and Par-Bri sites will in fact be identical.

Interestingly, we found that the C-adsorbed *h*-BN sheet and BNNTs are spin-polarized, with a net magnetic moment of $2.0\mu_B$ (Figure S1 in the Supporting Information) regardless of the tube size and type of adsorption structures (Figures 2 and 3). This is distinctly different from the case of C-adsorbed CNTs, where the magnitude of the magnetic moment ($0.20-0.44\mu_B$) is sensitively dependent on the adsorption geometry (i.e., the specific local bonding configuration of the adatom and the adjacent tube atoms) and the electronic structure of the tube (i.e., semiconducting or metallic).[12] We further checked the validity of the magnetic structures of the C-adsorbed BN nanostructures in the ground state by restricting the system to the paramagnetic ($S = 0$) state. The results show that for the (8,0) BNNTs with C adatoms at the Per-Bri and Par-Bri sites, the energies of the paramagnetic states are, respectively, 0.50 and 0.15 eV higher than those of the corresponding ferromagnetic ($S = 1$) states, while the energy of the paramagnetic state is 0.41 eV higher for the C-adsorbed *h*-BN sheet. More importantly, the ferromagnetic−paramagnetic energy difference is at least 4 times larger than that of C-adsorbed graphene (∼36 meV), which was believed to correspond to a Curie temperature of 100−200 K.[12] This indicates that *C adsorption on BN nanostructures* might provide nanoscale high-temperature ferromagnetic building blocks for spintronic devices with a stronger magnetism and a higher Curie temperature, making them superior to the C-based analogues.

Previous studies have shown that local magnetic moments in open-zigzag or C-substituted B(N) armchair BNNTs are mainly due to the unpaired valence electrons.[7] Comparatively speaking, the situation is more complicated in C-adsorbed BN nanostructures. From the point of view of orbital hybridization, we have elucidated the origin of the magnetism of C adatoms on BN nanostructures to be based on the localization of valence electronic states of the dopant, in comparison with the case of C adatoms on carbon nanostructures. In detail, bonding analysis with the local density of states (LDOS) shows that when the C atom is adsorbed on BNNTs (CNTs) or an *h*-BN sheet (graphene), among the four valence electrons of the C adatom, two electrons in sp^2 hybrid orbitals strongly interact with the electrons of adjacent host atoms, resulting in adsorption (see Figures 2 and 3), while the remaining sp^2 and p_z orbitals occupied by the other two electrons have different couplings to the states of the host. In general, whether the coupling occurs is closely related to the localization/delocalization of the states near the Fermi level of the host. The coupling directly affects the localization of impurity states and further determines the strength and stability of the induced magnetism. A representative example is that identical C adsorption would lead to distinctly different magnetic properties for BN tubes/sheets and their C-based analogues, as mentioned above.

It is well-known that for pristine BN tubes and sheets, the occupied and unoccupied π states near the Fermi level are highly

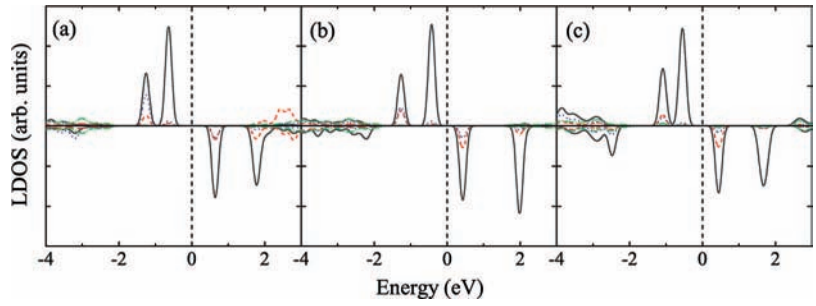

Figure 2. Spin-polarized LDOS for the (8,0) BNNT with the C adatom adsorbed at the (a) Per-Bri and (b) Par-Bri sites and (c) for the C-adsorbed SL *h*-BN sheet. Gray solid, red dashed, blue dotted, and green dash-dotted lines represent the LDOS of adsorbed C atoms, adjacent B and N atoms, and remaining host atoms, respectively. The Fermi level is set to zero energy.

localized but have different characteristics.[22] Typically, the highest occupied molecular orbital (HOMO) corresponds to isolated electron pairs localized at the N atoms, whereas the main contribution to the lowest unoccupied molecular orbital (LUMO) is comes from the B 2p orbital.[22] For the C-absorbed BN tubes and sheet, the LDOS (Figure 2) and molecular orbitals (Figure 3) show that the HOMO consists only of the p_z orbital of the C adatom, which is normal to the B−N−C plane, while the HOMO-1 is composed of the remaining sp^2 orbital of the C adatom and π orbitals of the two adjacent B and N atoms. Because of the curvature effect, the degree of this hybridization decreases in order of the C-adsorbed Per-Bri structure, the C-adsorbed Par-Bri structure, and the C-adsorbed SL *h*-BN sheet (as demonstrated by the second peaks of majority spin below the Fermi level in panels a, b, and c, respectively, of Figure 2). As a consequence of their high localization, the states of the adjacent B and N atoms play a "confinement" role for the remaining sp^2 states of the C adatom, and hence, the electron of this sp^2 hybrid orbital is confined in the same B−N−C plane (Figure 3b,d,f). Consequently, the HOMO and HOMO-1 are highly localized, and each contributes a magnetic moment of $1.0\mu_B$.

In contrast, in the C-adsorbed graphene and CNTs, the spin−charge density exhibits only the characteristics of a p_z orbital (see the inset of Figure 4), which is in agreement with the reported results.[12] From Figure 4, we can see that the local magnetic moment and the spin splitting between the majority- and minority-spin states are attributable to the partial localization of the p_z states of the C adatom, while the sp^2 states of the C adatom hybridize with not only the sp^2 orbitals of the adjacent two C atoms but also the π states of the host (Figure 4). Since the π states near the Fermi level of graphene and CNTs are nearly delocalized over the whole system, the strong coupling causes the electrons in the sp^2 orbitals to be delocalized. This facilitates the conductivity of semiconducting CNTs but hardly contributes to the magnetism.[12] As such, the localized p_z states of the C adatom couple to the delocalized π states of the host, showing the "shoulder-to-head" hybridization configuration (see the inset of Figure 4). As a result, the half-electron of the p_z orbital is delocalized and thus does not contribute to the magnetism. This well explains why the magnetic moment of C adsorbed on graphene or CNTs is less than $0.5\mu_B$.[12] The understanding of the coupling mechanism also provides a

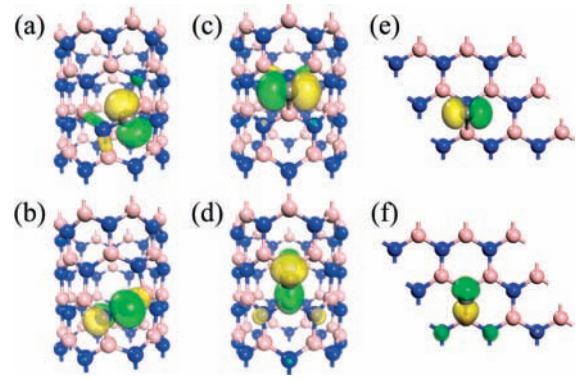

Figure 3. (a) [(c)] HOMO and (b) [(d)] HOMO-1 band states for the (8,0) BNNT with the C adatom adsorbed at the Per-Bri [Par-Bri] site; (e) HOMO and (f) HOMO-1 band states for the C-adsorbed SL *h*-BN sheet. The isosurfaces of the HOMO and HOMO-1 band states at the Γ point with values of 0.08 and −0.08 au are depicted in green and yellow, respectively.

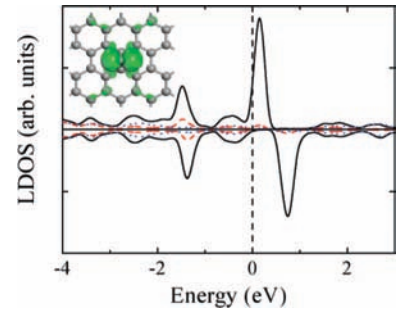

Figure 4. Spin-polarized LDOS for C-adsorbed graphene. Gray solid, red dashed, and blue dotted lines represent the LDOS of the adsorbed C atom, the adjacent two C atoms, and the remaining host C atoms, respectively. The Fermi level is set to zero energy. The isosurface for spin−charge density at a value of 0.005 e/Å^3 is shown in the inset.

perspective on the magnetism of sp-electron nanosystems induced by adatoms without any d electrons. It is expected that similar adatom-induced magnetism might emerge in other compound nanotubes or sheets, such as II−VI and other III−V semiconductors.

In general, the question of whether the local magnetic moments result in collective magnetism, which involves long-range magnetic coupling, is a crucial issue for applications. Therefore, we further explored the magnetic interactions between the C-induced magnetic moments on BN nanostructures. Taking the C-adsorbed (12,0) BNNT as an example, we found that when two C adatoms are initially placed in the same hexagonal ring of a BNNT, the local magnetic moment induced

(21) Chen, Y.; Hu, C.-L.; Li, J.-Q.; Jia, G.-X.; Zhang, Y.-F. *Chem. Phys. Lett.* **2007**, *449*, 149.
(22) (a) Khoo, K. H.; Mazzoni, M. S. C.; Louie, S. G. *Phys. Rev. B* **2004**, *69*, 201401. (b) Wu, X. J.; Yang, J. L.; Hou, J. G.; Zhu, Q. S. *Phys. Rev. B* **2004**, *69*, 153411. (c) Li, J.; Zhou, G.; Liu, H. T.; Duan, W. H. *Chem. Phys. Lett.* **2006**, *426*, 148.

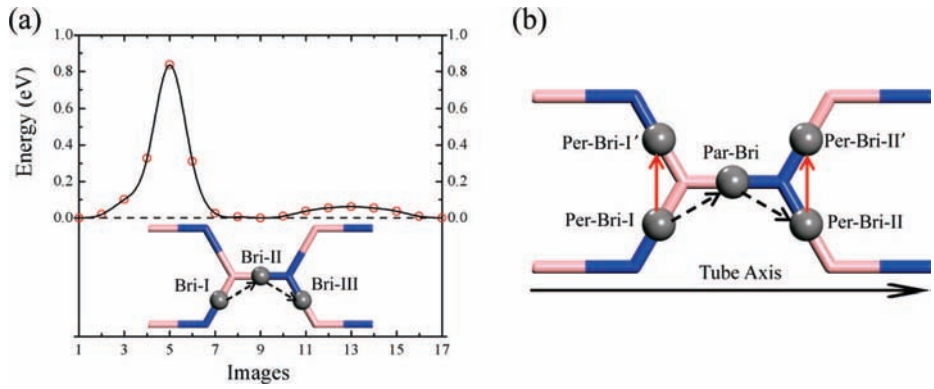

Figure 5. (a) Minimum-energy path for C-adatom diffusion among three equivalent bridge sites (Bri-I, Bri-II, and Bri-III) on an SL *h*-BN sheet. Black dashed arrows show the diffusion path. (b) Schematic illustration of C-adatom diffusion between different bridge sites on the outer surface of a BNNT. Black dashed (red solid) arrows show the diffusion path of C adatoms along the tube axis (circumference). It should be noted that all Per-Bri sites are equivalent to each other but different from the Par-Bri site.

by each C adatom is completely quenched as a result of the formation of a C dimer. The hybrid system is nonmagnetic. Next, we gradually increased the initial distance between two C adatoms along the tube axis and performed the structural relaxation. We found that the dimerization does not occur when two C adatoms are initially placed into two different BN hexagonal rings. Although every C adatom still has a magnetic moment of $2.0\mu_B$, the antiferromagnetic state is most stable for this system. Finally, when the distance between the two C adatoms is larger than 9.0 Å, the antiferromagnetic and ferromagnetic configurations of the C-adsorbed BNNT are nearly degenerate. A recent study showed that by injecting negative charges into the wide-gap group III nitrides (i.e., GaN) with cation vacancies, the stable states transform to the ferromagnetic configuration from the antiferromagnetic configuration.[23] Thus, it is expected that for the antiferromagnetic C-adsorbed BN nanostructures, a similar approach of injecting negative charges can be used to alter their ground-state properties. Our further calculations demonstrate that with the injection of two or more negative charges, C-adsorbed BN nanostructures with a C−C distance of 4.35 Å have the ferromagnetic state at a lower energy (i.e., the ferromagnetic−antiferromagnetic energy differences are 5, 9, and 12 meV for injection of two, three and four negative charges, respectively, which are comparable to those in GaN[23]), and collective magnetism of the systems appears as a result of the coupling between these local magnetic moments. However, the antiferromagnetic and ferromagnetic configurations of C-adsorbed BNNTs also become nearly degenerate with an increasing number of injected negative charges if the C−C distance is larger than 9.0 Å. The unusual magnetic properties mentioned here indicate the great potential of C-adsorbed BN nanostructures for use as high-temperature ferromagnetic semiconductors or as building blocks for spintronic devices.

For practical applications, it is also important to understand the stability of the magnetism of C-adsorbed BN nanostructures (especially at ambient temperature). To address this issue, we further studied the diffusion of C adatoms on BNNTs and *h*-BN sheets. Using the nudged elastic band (NEB) method,[24] we first calculated the minimum-energy path (MEP) for C-adatom diffusion among three equivalent bridge sites (Bri-I, Bri-II, and Bri-III) on an SL *h*-BN sheet. As shown in Figure 5a, the barrier for diffusion of the C atom across the B atom from Bri-I to Bri-II (0.86 eV) is far larger than that of the C atom across the N atom from Bri-II to Bri-III (0.06 eV). This is consistent with the fact that the interaction between C and N atoms is stronger than that between C and B atoms.[25] Successively, we calculated the diffusion barriers of the C adatom on the outer surfaces of (8,0) and (12,0) BNNTs using the LST/QST method.[19] Unlike the case of the *h*-BN sheet, the C adatom on a BNNT may diffuse along the tube axis and along the tube circumference (see Figure 5b). For the C adatom on the (8,0) BNNT, the barriers for diffusion from Per-Bri-I to Par-Bri (corresponding to the diffusion over the B atom) and from Par-Bri to Per-Bri-II (corresponding to diffusion over the N atom) are 1.03 and 0.36 eV, respectively. For the (12,0) BNNT, the corresponding diffusion barriers are 0.90 and 0.28 eV. The barriers for C-adatom diffusion on BNNTs are higher than those on *h*-BN and decrease with increasing tube diameter, as a consequence of the curvature effect. It is interesting to note that a similar trend was observed in the cases of C-adatom diffusion on CNTs and graphene,[12] but the barriers are lower for BNNTs than for CNTs with similar diameters. For C-adatom diffusion along the tube circumference (Figure 5b), the barriers for diffusion over the B and N atoms are 1.53 and 0.91 eV, respectively, for the (12,0) BNNT. This indicates that the C-adatom diffusion on the outer surface of BNNTs is anisotropic and occurs predominantly along the tube axis, facilitating the growth of heterostructured BN/C nanotubes. Under the barrier obtained above, the diffusion would occur easily at typical growth temperatures.[20] In view of the actual growth conditions, we can deduce that when the C atoms are adsorbed on as-grown BNNTs or an SL *h*-BN sheet, they can easily diffuse to the open ends of the BNNTs or the edges of the *h*-BN sheet. Hence, it is rather possible to fabricate heterostructured C/BN nanotubes or C/BN sheets (as shown in Figure 6a,b), consistent with the previous thermodynamic analysis of the growth of BN/C nanosystems.[1]

Our results for the adsorption and diffusion properties of C adatoms on BN nanostructures suggest that such hybrid systems can stably exist even with C diffusion, and the distribution of doped C atoms at the hosts can be changed by increasing or reducing the experimental temperature to drive the C adatom to the growing edge or not. Thus, we herein propose a method

(23) Dev, P.; Xue, Y.; Zhang, P. H. *Phys. Rev. Lett.* **2008**, *100*, 117204.
(24) (a) Mills, G.; Jonsson, H.; Schenter, G. K. *Surf. Sci.* **1995**, *324*, 305. (b) *Classical and Quantum Dynamics in Condensed Phase Simulations*; Berne, B. J., Ciccotti, G., Coker, D. F., Eds.; World Scientific: London, 1998.
(25) Yi, J.-Y.; Bernholc, J. *Phys. Rev. B* **1993**, *47*, 1708.

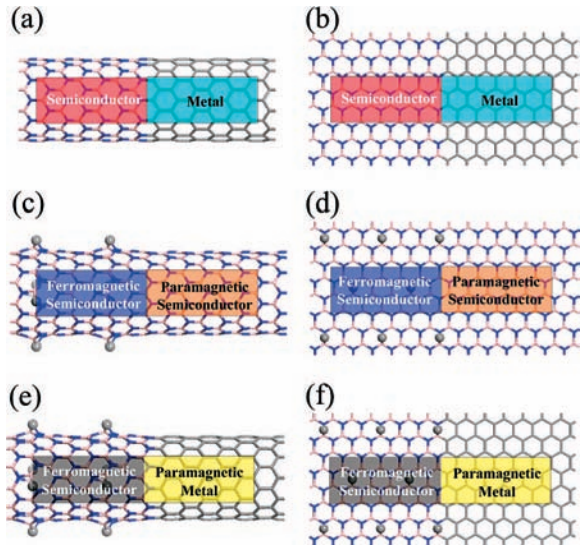

Figure 6. Schematic illustrations of six typical building blocks for functional devices: semiconductor−metal junctions between (a) a BNNT and a CNT and (b) an SL *h*-BN sheet and a graphene; ferromagnetic semiconductor−paramagnetic semiconductor junctions between (c) a C-adsorbed BNNT and a pristine BNNT and (d) a C-adsorbed SL *h*-BN sheet and a pristine SL *h*-BN sheet; and ferromagnetic semiconductor−paramagnetic metal junctions between (e) a C-adsorbed BNNT and a pristine CNT and (f) a C-adsorbed SL *h*-BN sheet and a pristine graphene.

for fabricating BN−C-based functional devices. In detail, at a low temperature where the C adatoms have difficulty in migrating, a spintronic device (e.g., spin valve or spin-polarization switch) could be formed by controlling the magnetism in the selective C-adsorbed BN nanosystems with the help of injection of negative charges or ionization of trapped holes, whereas the BN/C superlattices or heterojunctions can be grown by controllable C diffusion at a high or growth temperature. A series of typical building blocks for functional devices are illustrated in Figure 6. On the basis of these building blocks, one could integrate different types of electronic or spintronic devices (e.g., logic gates) used in computer science and information science.

IV. Summary

Using spin-polarized DFT calculations, we have found that single-C-atom adsorption on zigzag BNNTs and *h*-BN sheets leads to a net magnetic moment of $2.0\mu_B$. This unusual magnetic property is independent of the tube size and the bonding of the adatom to the adjacent host atoms and originates from the strong localization of the impurity states. Orbital hybridization is adopted to elucidate in detail the differences in induced magnetism in C-adsorbed BN and C nanostructures, which are attributed to different coupling mechanisms. The dependence of the interaction between C-induced magnetic moments along the tube axis on the distance between adatoms is demonstrated. By injecting negative charges, such hybrid systems can exhibit collective magnetism. In terms of calculated diffusion barriers and adsorption energies, a method (involving control of the experimental temperature to affect the C adsorption and migration) is proposed for fabricating BN−C-based functional devices, and some virtual building blocks for functional devices are illustrated.

Acknowledgment. This work was supported by the National Natural Science Foundation of China (Grants 10674077 and 10774084), the Ministry of Science and Technology of China (Grants 2006CB605105, 2006CB0L0601, and 2009CB929400), and the Linkage International Awards from the Australian Research Council.

Supporting Information Available: Spin−charge distributions of the C-adsorbed (8,0) BNNT and the C-adsorbed SL *h*-BN sheet. This material is available free of charge via the Internet at http://pubs.acs.org.

JA805632P